Pure nickel (nickel 200, UNS N02200, Ni99.6 DIN-Mat. No. 2.4060, Ni99.2 DIN-Mat. No. 2.4066) exhibit a certain resistance in dilute hydrochloric acid at room temperature. The attack is enhanced by aeration and the presence of oxidising agents in the acid.

A 27 Nickel-chromium alloys
A 28 Nickel-chromium-iron alloys (without Mo)

The molybdenum-free NiCr or NiCrFe alloys, e.g. NiCr16Fe (UNS N06600, Inconel® 600, Alloy 600, DIN-Mat. No. 2.4816) or NiCr21Fe (Inconel® 800), are not used in hydrochloric acid because in dilute solutions they are susceptible to pitting corrosion and in concentrated solutions at elevated temperatures they are also susceptible to general surface corrosion . Their corrosion resistance is lower than that of pure nickel or alloy 400. More information on the resistance of NiCr or NiCrFe alloys in hydrochloric acid is given in reference [47].

A 29 Nickel-chromium-molybdenum alloys

The nickel-chromium alloys used in chemical process engineering generally contain molybdenum as well to increase the pitting and crevice corrosion resistance. The most commonly used materials are given in Table 59 with the frequently used and familiar manufacturer's designations.

Manufacturer's designation	*UNS*	*DIN-Mat. No.*	*Abbreviation*
Incoloy® 825 Nicrofer® 4221 Alloy 825 Uranus® 825	N08825	2.4858	NiCr21Mo
Inconel® G-3 Alloy G-3 Nicrofer® 4823 hMo	N06985	2.4619	NiCr22Mo7Cu
Inconel® 625 Alloy 625 Nicrofer® 6020 hMo Uranus® 625	N06625	2.4856	NiCr22Mo9Nb
Alloy C 276 Hastelloy® C-276 Nicrofer® 5716 hMoW	N10276	2.4819	NiMo16Cr15W
Hastelloy® C-4 Alloy C-4 Nicrofer® 6616 hMo	N06455	2.4610	NiMo16Cr16Ti
Nicrofer® 5923 hMo Alloy 59	N06059	2.4605	NiCr23Mo16Al

Table 59: Nickel-chromium-molybdenum alloys frequently used in chemical process engineering

As the molybdenum content increases, the resistance of the NiCrMo alloys decreases in hydrochloric acid so that alloy 625 has a better resistance than alloy G-3, which in turn is more resistant than alloy 825.

As the isocorrosion diagram in Figure 61 shows for alloy 825, it can be expected that this material has insufficient resistance at low acid concentrations and temperatures [68].

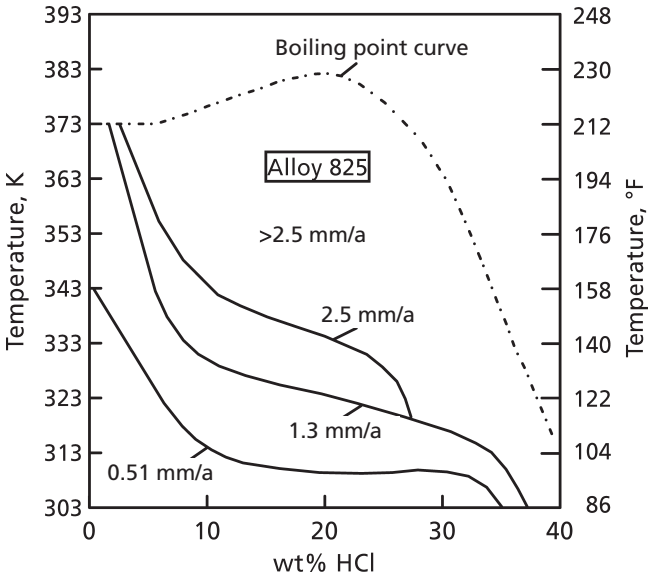

Figure 61: Isocorrosion diagram for alloy 825 in hydrochloric acid [68, p. 32]
> 2.5 mm/a (> 100 mpy)
2.5 mm/a (100 mpy)
1.3 mm/a (50 mpy)
0.51 mm/a (20 mpy)

The isocorrosion diagrams for alloy G-30 (UNS N06030, a modified G-3 variant) in Figure 62, alloy C-276 in Figure 63, alloy C-4 in Figure 64 and alloy 59 in Figure 65 demonstrate the considerably improved behavior of these materials [68].

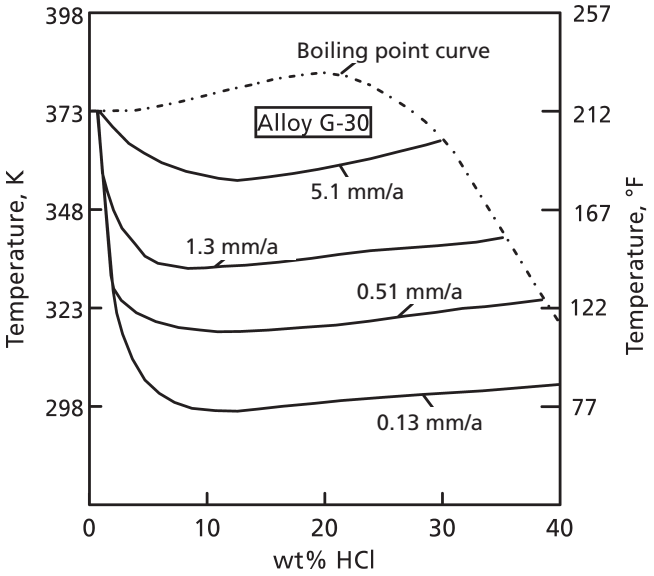

Figure 62: Isocorrosion diagram for alloy G-30 in hydrochloric acid [68, p. 33]
5.1 mm/a (200 mpy)
1.3 mm/a (50 mpy)
0.51 mm/a (20 mpy)
0.13 mm/a (5 mpy)

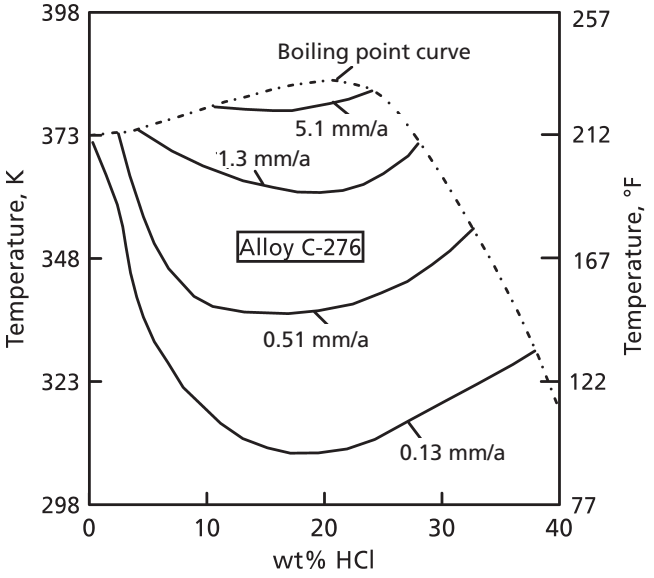

Figure 63: Isocorrosion diagram for alloy C-276 in hydrochloric acid [68, p. 34]
5.1 mm/a (200 mpy)
1.3 mm/a (50 mpy)
0.51 mm/a (20 mpy)
0.13 mm/a (5 mpy)

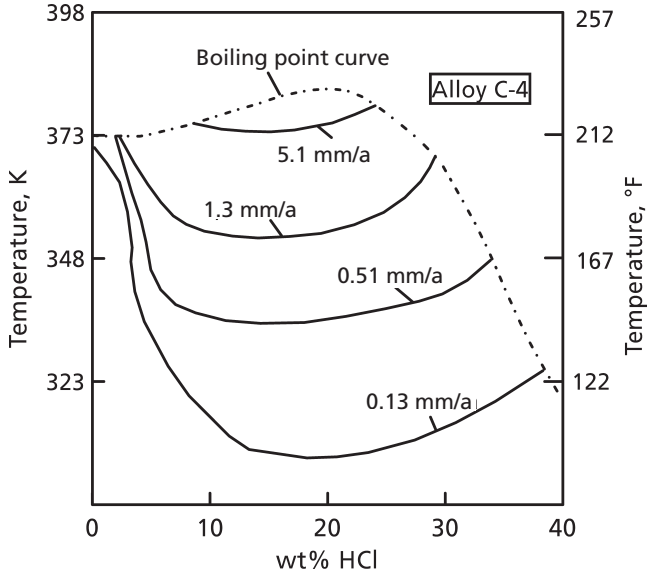

Figure 64: Isocorrosion diagram for alloy C-4 in hydrochloric acid [68, p. 36]
5.1 mm/a (200 mpy)
1.3 mm/a (50 mpy)
0.51 mm/a (20 mpy)
0.13 mm/a (5 mpy)

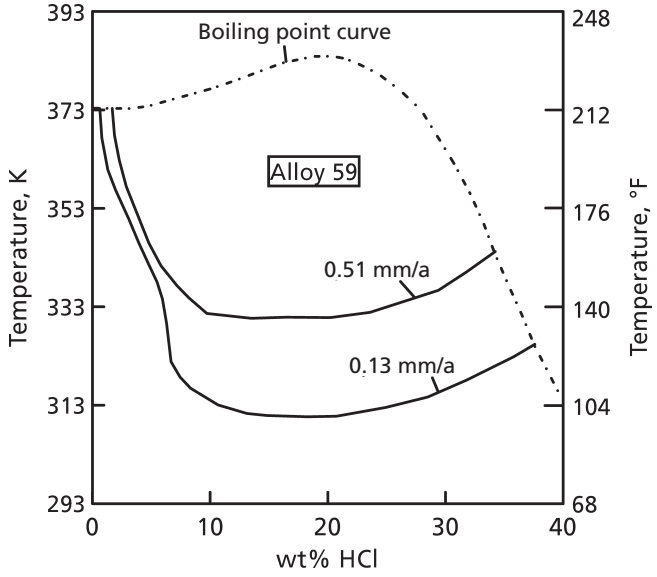

Figure 65: Isocorrosion diagram for alloy 59 in hydrochloric acid [68, p. 39]
0.51 mm/a (20 mpy)
0.13 mm/a (5 mpy)

Reference [93] discusses the factors that led to the development of the Ni-Cr-Mo-W alloy Hastelloy® C-22 (UNS N06022). Compared to other nickel-based alloys, it exhibits a very high corrosion resistance both in very aggressive reducing and oxidising acids.

Table 60 gives the composition of alloys in the development sequence of alloys developed prior to alloy C-22. During welding of alloy C with max. 0.08 % C and max. 1.0 % Si, chromium carbides were precipitated on the grain boundaries in the substrate material next to the weld seam, making this zone susceptible to intergranular corrosion. Therefore, the utilisation of this material was greatly limited because a subsequent solution annealing and quenching to eliminate the susceptible zones was only possible to a limited extent.

Alloy	*Cr*	*Mo*	*W*	*Fe*	*Nb*	*Ti*	*V*	*Mn*	*C*	*Si*	*Ni*
Alloy C	15	16	4	5	–	–	0.35 (1)	1.0 (1)	0.08 (1)	1.0 (1)	balance
Alloy C-276	16	16	4	5	–	–	0.35 (1)	1.0 (1)	0.01 (1)	0.08 (1)	balance
Alloy C-4	16	16	–	3 (1)	–	0.70 (1)	–	1.0 (1)	0.01 (1)	0.08 (1)	balance
Alloy C-22	22	13	3	3	–	–	0.35 (1)	0.50 (1)	0.015 (1)	0.08 (1)	balance
Alloy 625	21.5	9	–	5.0 (1)	3.5	0.40 (1)	–	0.5 (1)	0.10 (1)	0.50 (1)	balance
Alloy HC new	20	15	–	2	–	–	–	–	0.01	0.03	balance

(1) Maximum

Table 60: Composition of the Ni-Cr-Mo/W alloys, mass% [93]

By reducing the carbon content to max. 0.01 % and the silicon content to 0.08 %, intergranular susceptibility was eliminated in alloy C-276 [94]. In spite of its excellent general corrosion resistance, this alloy is still somewhat susceptible to preferred attack in the welding seam and in the heat-affected zone of the welded material because in the temperature range from 973 to 1373 K (700 to 1100 °C) a chromium and molybdenum-rich intermetallic phase (μ-phase) can be precipitated that is also susceptible to intergranular corrosion in aggressive acids.

Alloy C-4 was developed at a later date. This tungsten-free alloy with a reduced iron content is particularly thermally stable. An intermetallic phase is precipitated only after 100 h in the temperature range from 923 to 1373 K (650 to 1100 °C). The intergranular susceptibility due to precipitation of carbides is avoided by the low carbon content and by stabilisation with titanium. However, due to the lack of tungsten, the resistance to local corrosion (pitting and crevice corrosion) is reduced. Additionally, the resistance to oxidising acids is limited.

The increasing understanding of the effect of the individual alloying elements on the corrosion behavior allows the development of alloys with optimum corrosion properties. In nickel-based alloys, chromium enhances the resistance in oxidising acids, whereas molybdenum and tungsten enhances that in reducing acids. Based on this knowledge, the atomic percent factor (APF) was developed in order to compare the corrosion resistance of alloys with differing compositions. It expresses the opposing effect of chromium compared to that of molybdenum and tungsten. The ratios of the atomic weights of the relevant elements are

Cr (52) : Mo (96) : W (184) = 1 : 2 : 4

The APF is defined as the ratio of four times the weight% of chromium to the sum of twice the weight% of molybdenum + one times the weight% of tungsten, namely

APF = 4 Cr/(2 Mo + 1 W).

A high APF indicates a high resistance to oxidising acids, whereas a low APF indicates a high resistance to reducing acids. For an intermediate value of 2.5 to 3.3, the resistance to oxidising as well as reducing acids is high. The ratios are represented graphically in Figure 66. Alloy C-22 has an APF ≈ 3, which is the most favorable composition with respect to the corrosion behavior in oxidising and reducing acids.

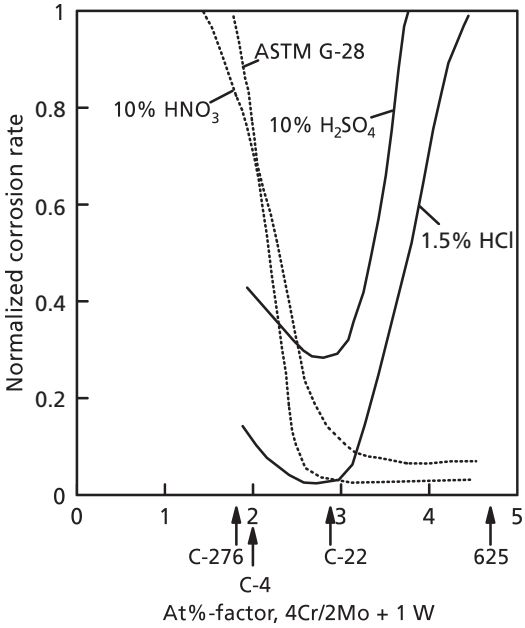

Figure 66: Range of optimum resistance in reducing and oxidising environments [93]

C-22 has a higher thermal stability than C-276. On tempering at 1200 K (927 °C), the temperature at which the fastest precipitation of the intermetallic phase occurs, intergranular susceptibility starts in less than 2 min for C-276, and in less than 15 min for C-22.

Table 61 gives comparative corrosion rates of the alloys listed in Table 60 in oxidising and reducing acidic aggressive media. Alloy C-22 exhibited the highest corrosion resistance in all media.

Alloy C-22 also exhibited the highest resistance in pitting and crevice corrosion tests in the $FeCl_3$ test with increasing temperature [95]. The lower molybdenum content compared to alloy C-276 is more than overcompensated by the higher chromium content.

Acid mixture	Temperature K (°C)	C-22	C-276	C-4	625
5 % HNO_3 + 6 % HF	333 (60)	1.68 (66.14)	5.18 (203.94)	5.1 (200.79)	1.825 (71.85)
5 % HNO_3 + 1 % HCl	boiling	0.0125 (0.49)	0.2 (7.87)	0.275 (10.83)	0.025 (0.98)
5 % HNO_3 + 25 % H_2SO_4 + 4 % NaCl	boiling	0.3 (11.81)	1.6 (62.99)	2.425 (95.47)	17.83 (701.97)
23 % H_2SO_4 + 1.2 % HCl + 1 % $FeCl_3$ + % $CuCl_2$	boiling	0.175 (6.89)	1.375 (54.13)	57.35 (2,257.87)	96.18 (3.786,61)

Table 61: Corrosion rates under oxidising conditions, mm/a (mpy) [93]

Even in the stress corrosion cracking tests, C-22 was generally better than alloys C-276 and 625 in aggressive media that trigger stress corrosion cracking.

However, as the values in Table 62 show for pure hydrochloric acid, the corrosion rates of alloy 59 and alloy C-276 were lower than those of alloy C-22 [68].

Acid concentration %	Temperature K (°C)	Corrosion rate mm/a (mpy)		
		C-22	C-276	59
1.5	Boiling	0.87 (34.2)	0.69 (27.2)	0.38 (14.9)
2	363 (90)	0.051 (2.01)	0.53 (20.8)	0.00 (0.0)
2	Boiling	2.18 (85.8)	1.14 (44.9)	0.99 (39)
3	363 (90)	1.41 (55.5)	0.96 (37.8)	0.053 (2.1)
3	boiling	4.55 (179)	2.06 (81.1)	2.05 (80.7)
5	366 (93)	5.07 (200)	1.99 (78.4)	2.81 (110.6)
10	328 (55)	0.77 (30.3)	0.44 (17.3)	0.55 (21.7)
10	355 (82)	3.03 (119)	1.56 (61.4)	2.47 (97.2)
10	Boiling	9.26 (365)	6.07 (239)	7.50 (295)

Table 62: Corrosion rates of the NiCrMo alloys C-22, C-276 and 59 in hydrochloric acid of differing concentrations and temperatures [68]

Acid mixtures

Acid mixtures are frequently used in chemical and metallurgical processes. For example, mixtures of nitric acid and hydrofluoric acid are used to pickle stainless steels. Although there have been many publications on the corrosion behavior of many alloys in pure acids, not enough is known about the corrosion behavior in mixed acids. Reference [96] reports on the corrosion behavior of nickel-based alloys in mixed acids. The results are based on the determination of the mass loss rates in static solutions that have not been deaerated.

Alloy	UNS No.	Fe	Cr	Ni	Mo	C	Others
AISI 316 L (corresp to. DIN-Mat. No. 1.4404)	S31603	balance	17	12	2.5	0.93	–
Ferrallium® Alloy 255 (corresp to. DIN-Mat. No. 1.4492)	S32550	balance	26	5.5	3.0	0.04 (1)	Cu = 1.7 N = 0.2
Alloy C-276	N10276	5.0 (1)	16	balance	16	0.01 (1)	W = 4.0
Alloy C 22 (corresp to. DIN-Mat. No. 2.4602)	N06022	3.0	22	balance	13	0.015 (1)	W = 3
Alloy G-3 (corresp. to DIN-Mat. No. 2.4619)	N06985	20	22	balance	7	0.015 (1)	Cu = 2.0 Nb = 0.5(1)
Hastelloy® Alloy G-30 (corresp to. DIN-Mat. No. 2.4603)	N06030	15	29.5	balance	5	0.3 (1)	Nb = 0.7 W = 2.5 Cu = 1.7
Alloy B-2 (corresp to. DIN-Mat. No. 2.4617)	N10665	2.0 (1)	1.0 (1)	balance	28	0.02 (1)	–

(1) Minimum

Table 63: Composition of the investigated alloys, mass% [96]

Table 63 gives the maximum chemical composition of the investigated alloys in mass%. For comparison purposes, the stainless steel AISI 316 L (1.4404) and the duplex steel Ferallium® Alloy 255 were also included.

Nickel-based alloys exhibited high corrosion rates, particularly in strongly reducing acids. They are designed for such operating conditions. The corrosion rate is more or less strongly increased if oxidising media are also present. Therefore, it is particularly important to determine the corrosion behavior of these materials in acid mixtures.

Figure 67 gives the isocorrosion curves for alloy Hastelloy® C-276 at 353 K (80 °C) in the three-component representation H_2O – HCl – HNO_3. The data are limited to one corner of the triangular representation because the maximum concentrations of the analytical grade acids used was 71 % for HNO_3 and 38 % for HCl. This form of representation shows the corrosion behavior of an alloy in a wide range of acid combinations; however, it is not very suitable for a comparison of the corrosion behavior of different alloys. Further results are thus given as a function of the proportion of an acid in another acid of constant concentration.

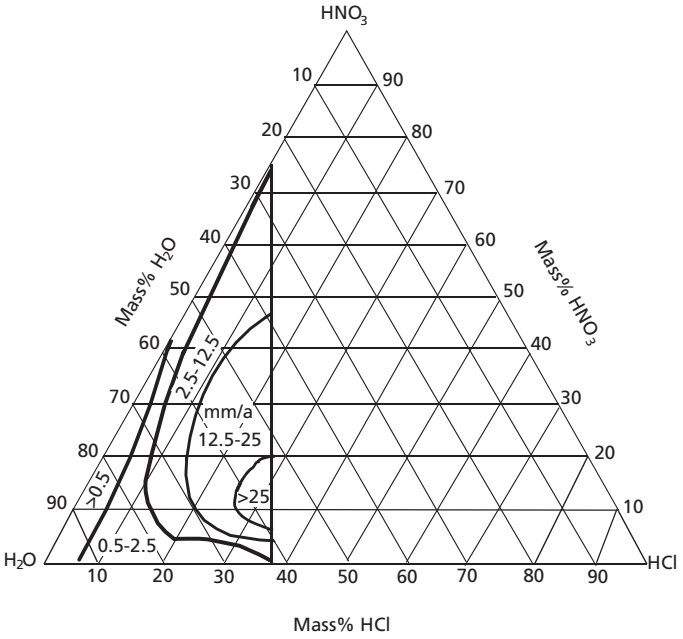

Figure 67: Isocorrosion curves for the alloy Hastelloy® C-276 at 353 K(80 °C) in the three-component representation H_2O – HCl – HNO_3 (175 °F) [96]

< 0.5 mm/a (< 20 mpy)
0.5-2.5 mm/a (20-100 mpy)
2.5-12.5 mm/a (100-500 mpy)
12.5-25 mm/a (500-1000 mpy)
> 25 mm/a (1000 mpy)

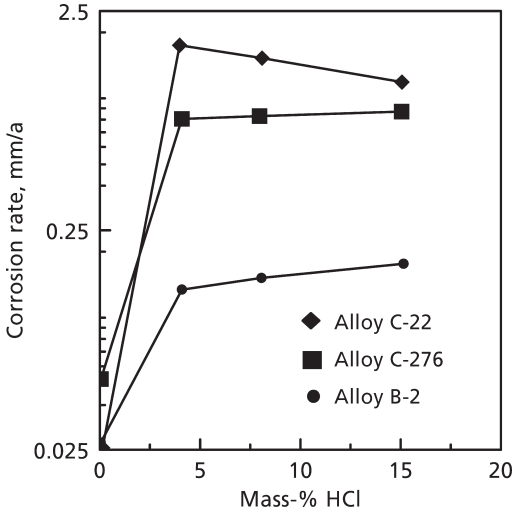

Figure 68: Corrosion rates of the alloys in 15 % H_2SO_4 at 80 °C (175 °F) [96]
(1 mm/a ≙ 39.37 mpy)

Figure 68 gives the corrosion rates of alloys C-22, C-276 and B-2 in 15 % H_2SO_4 at 353 K (80 °C) with increasing HCl concentration. Due to the reducing effect of hydrochloric acid, the corrosion rate increases by differing amounts, and increases more strongly with decreasing Mo content in the alloy. The attack is in the form of pitting corrosion.

On the other hand, with respect to the favorable behavior of B-2 in this mixture of two reducing acids, it must be pointed out that the corrosion resistance of this alloy is reduced in the presence of oxidising media, e.g. Fe^{3+} ions which are frequently present.

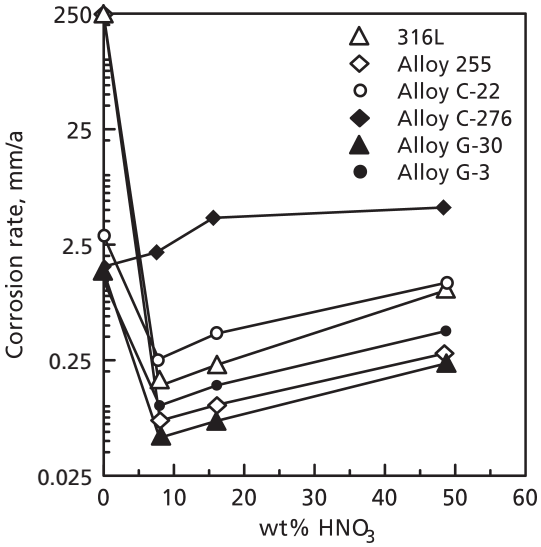

Figure 69: Corrosion rates in boiling 30 % H_2SO_4 with increasing concentration of HNO_3 [96] (1 mm/a ≙ 39.37 mpy)

With the exception of C-276, the addition of approx. 10 % of oxidising nitric acid to boiling 30 % H_2SO_4, a reducing acid, led to a large reduction in the corrosion rate, as shown in Figure 69. The effect is particularly large for the stainless steels AISI 316 L (1.4404) and Ferralium® Alloy 255, which are strongly attacked by boiling 30 % H_2SO_4. The corrosion rate is decreased by almost four powers of ten. If the HNO_3 concentration is increased further, then the corrosion rate increases again. In this range, the value of the corrosion rate is mainly determined by the amount of chromium and molybdenum contained in the alloy. The corrosion rate decreases with increasing chromium content and decreasing molybdenum content. Alloy C-276, with the lowest chromium (16 %) and highest molybdenum contents (16 %) has the highest corrosion rate and shows abnormal behavior. Alloy B-2 with 28 % Mo was not included in the investigation.

The addition of HNO_3 to 4 % HCl at 353 K (80 °C) leads to results, that are comparable to those in systems with boiling 30 % H_2SO_4 + HNO_3 (Figure 69 and Fig-

ure 70). There is a corrosion minimum for 10 % HNO_3. For further addition there is a stronger increase, whereby the level of the corrosion rate corresponds to the sequence in Figure 69, namely, the same alloying relationships are decisive for the corrosion rate. The attack is of the pitting type.

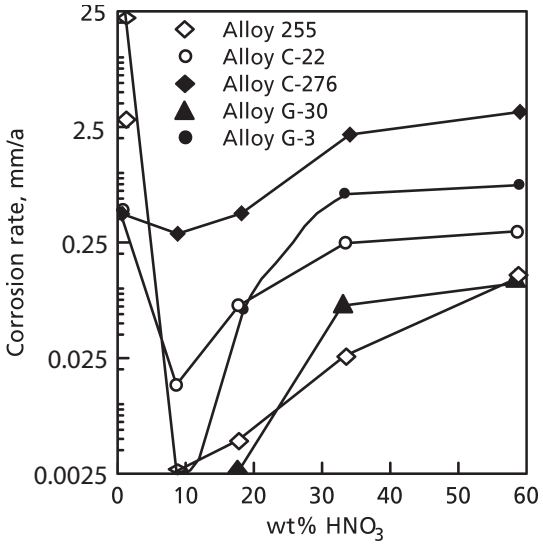

Figure 70: Corrosion rate in a 4 % HCl solution with increasing HNO_3 concentration at 80 °C (175 °F) [96]
(1 mm/a ≙ 39.37 mpy)

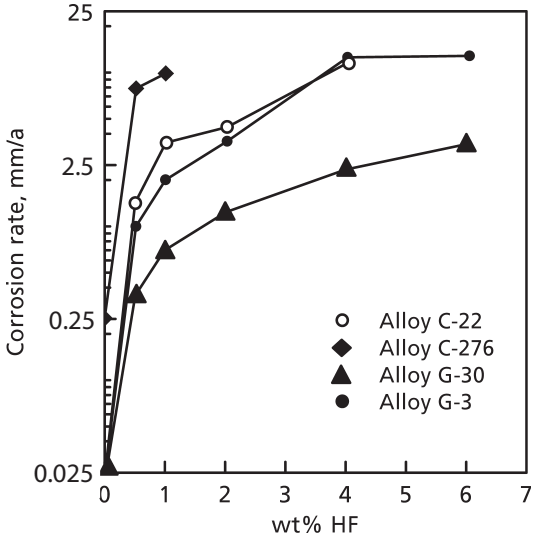

Figure 71: Corrosion rate in a 20 % HNO_3 solution with increasing HF concentration at 80 °C (175 °F) [96]
(1 mm/a ≙ 39.37 mpy)

To supplement the results, those for the nitric acid – hydrofluoric acid system are also given (Figure 71). This system is important for the pickling of stainless steels. The addition of HF to 20 % HNO_3 at 353 K (80 °C) gives a large continual increase of the corrosion rate already commencing at 1 % HF, whereby the sequence with respect to the high chromium and low molybdenum contents also applies.

High-performance alloys

Although extensive corrosion data is available for long-used stainless steels, there is still a lack of corresponding data for the "high-performance alloys". These include corrosion-resistant NiCr alloys with relatively high molybdenum content of up to approx. 30 % for the chemical process industry and superalloys for the gas turbine industry. The work in reference [97] reports on the nickel-based alloys given in Table 64, the corrosion resistant alloys Ferralium® Alloy 255, Haynes® No. 20-Mod. and, for purposes of comparison, the stainless steels AISI 304 (X5CrNi18-10, DIN-Mat. No. 1.4301) and AISI 316 L (X2CrNiMo17-12-2, DIN-Mat. No. 1.4404).

	Ni	*Fe*	*Cr*	*Mo*	*W*	*Co*	*Others*
Hastelloy® Alloy G	bal.	19.5	22	6.5	< 1	< 2.5	Cu-2, Nb + Ta-2
Haynes® Alloy No. 625	bal.	5	21.5	9	–	< 1	Nb + Ta-3.5
Hastelloy® Alloy C-276	bal.	5	16	16	4	< 2.5	V-0.35
Hastelloy® Alloy B	bal.	5	< 1	28	–	< 2.5	–
Hastelloy® Alloy B-2	bal.	< 2	< 1	28	–	< 1	low carbon content
Ferralium® Alloy 255	5	bal.	25.5	3.5	–	–	Cu-1.7, N-0.17
Haynes® Alloy No. 20-Mod.	26	bal.	22	9	–	–	Ti-4×C Min.
AISI 304	9	bal.	19	–	–	–	–
AISI 316 L	12	bal.	17	2.5	–	–	low carbon content

Table 64: Composition of the alloys, mass% [97]

The corrosion rates in various acids, obtained from measurements of the mass losses, are summarised in Table 65. As expected, the highest corrosion rates were found in boiling 10 % HCl, the most strongly reducing acid. By far the highest corrosion resistance was exhibited by B-2 in hydrochloric acid. In contrast, it had the lowest resistance by far in boiling 10 % HNO_3. As already found in other work, the level of molybdenum is decisive for the corrosion behavior in hydrochloric acid, whereas the level of the Cr content is decisive in nitric acid.

Alloys	*10% HCl*	*10% H_2SO_4*	*10% HNO_3*	*99% CH_3COOH*	*40% HCOOH*	*88% HCOOH*	*55% H_3PO_4*	*85% H_3PO_4*
Hastelloy® Alloy G	28.85 (1,136)	0.635 (25)	0.02 (0.79)	0.041 (1.61)	0.13 (5.12)	0.109 (4.29)	0.099 (3.9)	0.686 (27.01)
Haynes® Alloy No. 625	12.9 (508)	0.168 (6.61)	0.025 (0.98)	0.01 (0.39)	0.185 (7.28)	0.236 (9.29)	0.114 (4.49)	1.803 (70.98)
Hastelloy® Alloy C-276	5.7 (224)	0.584 (22.99)	0.432 (17.01)	0.01 (0.39)	0.074 (2.91)	0.046 (1.81)	0.071 (2.8)	0.508 (20)
Hastelloy® Alloy B-2	0.175 (6.89)	0.046 (1.81)	490.5 (19,311)	0.03 (1.18)	0.011 (0.43)	0.015 (0.59)	0.091 (3.58)	0.102 (4.02)
Ferralium® Alloy 255	478.2 [(1)] (18,827)	7.04 (277.17)	0.048 (1.89)	0.03 (1.18)	0.196 (7.72)	0.965 (37.99)	0.130 (5.12)	44.35 (1,746)
Haynes® Alloy No. 20-Mod.	281.2 (11,071)	4.45 (175.2)	0.015 (0.59)	0.018 (0.71)	0.356 (14.02)	0.711 (27.99)	0.279 (10.98)	10.62 (418.11)
AISI 316 L	449.2 [(1)] (17,685)	60.88 (2,397)	0.053 (2.09)	0.097 (3.82)	1.067 (42.01)	0.483 (19.02)	0.201 (7.91)	16.38 (644.88)

[(1)] Sample dissolved

Table 65: Corrosion rates (in boiling media), mm/a (mpy) [97]

The degree of corrosion resistance of Hastelloy® Alloy B-2 is not negatively influenced by cold deformation and welding. Table 66 shows that for cold forming of up to 50 %, cold forming with subsequent welding as well as cold forming after welding, the corrosion rate remained < 0.25 mm/a (< 10 mpy).

State	*mm/a (mpy)*	*State*	*mm/a (mpy)*	*State*	*mm/a (mpy)*
0 % cold-formed	0.165 (6.5)	0 % cold-formed + welded	0.165 (6.5)	welded + 0 % cold-formed	0.155 (6.1)
10 % cold-formed	0.133 (5.24)	10 % cold-formed + welded	0.188 (7.4)	welded + 10 % cold-formed	0.138 (5.43)
30 % cold-formed	0.145 (5.71)	30 % cold-formed + welded	0.235 (9.25)	welded + 30 % cold-formed	0.14 (5.51)
50 % cold-formed	0.108 (4.25)	50 % cold-formed + welded	0.155 (6.1)	welded + 50 % cold-formed	0.15 (5.91)

Table 66: Corrosion rates for Hastelloy® Alloy B-2 in 10 % HCl [97]

Furthermore, this work also investigated the behavior of the alloys with regard to types of local corrosion, namely pitting, crevice and stress corrosion cracking. For passive materials, the level of the chromium and molybdenum contents is decisive for the resistance to pitting and crevice corrosion. These types of corrosion are caused by chloride ions, and the presence of any oxidising agents enhances the effect. A 10 % $FeCl_3$ solution is generally used to test for pitting and crevice corrosion of stainless and chemically resistant steels. However, this test solution is not aggressive enough for nickel-based alloys that often contain large amounts of molybdenum. To test the pitting corrosion of nickel-based alloys, a solution consisting of 7 vol% H_2SO_4 + 3 vol% HCl + 1 % $FeCl_3$ + 1 % $CuCl_2$ was used to simulate the conditions in scrubbers. Table 67 gives the results of samples with artificial crevices and of samples that are not in contact with another body. In both test solutions, and also at the higher temperatures of 323 and 375 K (50 and 102 °C), C-276 did not exhibit either pitting or crevice corrosion because of its high pitting index of almost 70 (calculated according to W = % Cr + 3.3 x % Mo). It must be mentioned at this point that in the presence of crevices, crevice corrosion always occurs before pitting corrosion. The samples become active in the crevice, and pitting corrosion on the surface is prevented because of cathodic protection by the anodic crevice region. The results in Table 67 confirm this fundamental corrosion mechanism for passive materials.

The author of [97] gives a very detailed report on the testing of local corrosion of nickel-based alloys in reference [98]. In addition to the materials given in Table 64 [97], the alloy Incoloy® 825 with the nominal percentage composition 42 % Ni, 39 % Fe, 21 % Cr, 3 % Mo, max. 1 % Mn, max. 0.5 % Si, max. 0.05 % C, 0.8 % Ti, 2 % Cu was included in the investigation. The main aim was to correctly determine the "critical pitting corrosion potential" using electrochemical methods because this potential (if correctly measured) would allow a reliable comparison of the pitting corrosion behavior of various materials in one medium. The difficulty concerned with the

premature appearance of crevice corrosion on covers must be pointed out as it prevents the correct determination of the critical pitting corrosion potential. In addition, it is shown that the potentiodynamic quick test with a ramping rate of 1000 mV/min, which is often used, does not allow differentiation of the pitting corrosion behavior, particularly of the nickel-based alloy.

	10 % $FeCl_3$; Sample with artificial crevice		*Smooth samples 24 h 7 vol% H_2SO_4 + 3 vol% HCl + 1 % $FeCl_3$ + 1 % $CuCl_2$*	
Alloy	***25 °C (77 °F) 240 h***	***50 °C (122 °F) 100 h***	***25 °C (77 °F)***	***102 °C (215 °F)***
Hastelloy® Alloy G	0.4 [15.8]	0.575 [22.6] (crevice corrosion)	0.01 [0.39]	43.95 [1,730] (pitting corrosion)
Haynes® Alloy No. 625	0.038 [1.50]	3.1 [122.1] (crevice corrosion)	0.008 [0.31]	47.3 [1,862] (pitting corrosion)
Hastelloy® Alloy C-276	0.005 [0.20]	0.005 [0.20] (crevice corrosion)	0.008 [0.31]	0.6 [23.6]
Ferralium® Alloy 255	0.015 [0.59]	19.95 [785.4] (crevice corrosion)	0.003 [0.12]	75.4 [2,968] (pitting corrosion)
Haynes® Alloy No. 20-Mod.	0.105 [4.13]	2.35 [92.5] (crevice corrosion)	0.058 [2.3]	57.95 [2,281] (pitting corrosion)
AISI 316 L	7.8 [307.1] (crevice corrosion)	11.5 [452.8] (crevice corrosion)	2.53 [100.8] (pitting corrosion)	97.73 [3,848] (pitting corrosion)

Table 4 [68], p. 35

Table 67: Corrosion rates, mm/a [mpy] [97]

The work focused on potentiostatic holding tests with holding times of 24 h for each potential step of 100 mV, from – 200 mV to + 800 mV, measured against a saturated calomel electrode. The sample was checked for local corrosion (pitting and/or crevice corrosion) after every holding test. For practical applications, this is a damage limit, regardless of whether one or the other type of corrosion occurs. Table 68 summarises the results of the 24 h holding tests in five different solutions at 343 K (70 °C) for Hastelloy® G. The shaded area represents the region of the free corrosion potential. The acidic and at the same time oxidising solutions of columns 1 and 3 are suitable as test solutions for nickel-based alloys because their corrosion potential, due to a high redox potential of the solution, is polarised to the damage potential, whereas the corrosion potentials of the three other solutions without oxidising agents are more or less negative and lie below the corresponding danger potential.

U_{SCE} mV	7 vol% H_2SO_4 + 3 vol% HCl + 1 % $CuCl_2$ + 1 % $FeCl_3$ (pH ≈ 0.2)	1 vol% HCl + 3.8 % NaCl (pH ≈ 1.2)	3.8 % $FeCl_3$ (pH ≈ 1.3)	4 % NaCl (pH ≈ 5.5)	3 % Na_2SO_3 + 3 % $Na_2S_2O_5$ + 4 % NaCl (pH ≈ 12)
+ 800	*	*	*	*	o
+ 700	*	*	*	*	o
+ 600	*	*	*	*	o
+ 500	*	*	*	*	o
+ 400	*	*	*	*	o
+ 300	o	*	*	*	o
+ 200	o	*	o	*	o
+ 100	o	o	o	*	o
0	o	o	o	o	o
– 100	o	o	o	o	o
– 200	o	o	o	o	o

* = local corrosion; o = no local corrosion

Table 68: Hastelloy® alloy G; Results of the 24 h holding tests in five different solutions at 70 °C (158 °F) [98]

Table 69 gives the potential ranges for damage or resistance of all investigated materials in a 3.8 % $FeCl_3$ solution at 343 K (70 °C), determined with long-term potentiostatic tests. The resistance ranges are extended to more noble potentials as the molybdenum content in the alloys increases. This result agrees with theoretical and practical findings and confirms the serviceability of this test method.

U_{SCE} mV	2 to 3 % Mo AISI 316	3 % Mo Incoloy® Alloy 825	6.5 % Mo Hastelloy® Alloy G	9 % Mo Haynes® Alloy 625	16 % Mo Hastelloy® Alloy C-276
+ 800	*	*	*	*	o
+ 700	*	*	*	*	o
+ 600	*	*	*	*	o
+ 500	*	*	*	o	o
+ 400	*	*	*	o	o
+ 300	*	*	*	o	o
+ 200	*	*	o	o	o
+ 100	*	*	o	o	o
0	*	*	o	o	o
– 100	*	o	o	o	o
– 200	o	o	o	o	o

* = local corrosion; o = no local corrosion

Table 69: 24 h exposure at constant voltage in 3.8 % $FeCl_3$ solution at 70 °C (158 °F) [98]

In reference [99], the comparative corrosion resistance of alloys 625, C-276, Hastelloy® alloy C-22 and ALLCORR® was determined in HCl, H_2SO_4 and formic acid, the last two partly with low additions of HCl, HF, $FeCl_3$ and $CuCl_2$, at differing concentrations and temperatures over a test period of 48 h. The tolerance range for the composition of the alloys and the actual contents of the elements are summarised in Table 70. Welded samples were used that were prepared using the filling wires and welding conditions recommended by the manufacturers. The reason for the investigation was to select suitable materials for handling highly radioactive waste solutions, some of which are exceptionally corrosive.

	Alloy 625 (UNS N06625)	*Alloy C-276 (UNS N10276)*	*Hastelloy® Alloy C-22 (UNS N06022)*	*ALLCORR® (UNS N06110)*
Ni	60.20 (balance)	56.42 (balance)	57.52 (balance)	56.03 (balance)
Cr	22.34 (20.0-23.0)	16.11 (14.5- 16.5)	21.31 (20.0-22.5)	30.93 (27.0-33.0)
Mo	8.48 (8.0-10.0)	15.99 (15.0-17.0)	13.55 (12.5-14.5)	9.97 (8.0-12.0)
W	– (–)	3.85 (3.0-4.5)	3.17 (2.5-3.5)	1.97 (4.0 max.)
Fe	4.53 (5.0 max.)	5.76 (4.0-7.0)	3.52 (2.0-6.0)	0.11 (–)
C	0.04 (0.10 max.)	0.002 (0.02 max.)	0.003 (0.015 max.)	0.030 (0.15 max.)
To	0.25 (0.40 max.)	– (–)	– (–)	0.24 (1.5 max.)
Nb (+ Te)	3.51 (3.15-4.15)	– (–)	– (–)	0.42 (2.0 max.)
P	0.010 (0.015 max.)	0.004 (0.030 max.)	0.007 (0.02 max.)	0.005 (–)
Al	0.14 (0.40 max.)	– (–)	– (–)	0.23 (1.50 max.)
Si	0.34 (0.50 max.)	0.03 (0.08 max.)	0.021 (0.08 max.)	0.02 (–)
V	0.001 (0.015 max.)	0.002 (0.030 max.)	0.002 (0.02 max.)	0.001 (–)
Mn	0.16 (0.50 max.)	0.47 (1.0 max.)	0.21 (0.50 max.)	0.01 (–)
Co	– (–)	1.22 (2.5 max.)	0.52 (2.5 max.)	0.01 (12.0 max.)
Cu	– (–)	– (–)	0.07 (–)	0.01 (–)
V	– (–)	0.14 (0.35 max.)	0.01 (0.35 max.)	0.01 (–)

Numbers in brackets give the maximum content or the possible fluctuation

Table 70: Composition, mass% [99]

Solution (1)	%	Temperature °C (°F)	Alloys	Corrosion rate (µm/a)
HCl	35	84 (183)	625	28,000
			C-276	4,100 (2)
			C-22	6,800 (2)
			ALLCORR®	7,900 (2), (3)
HCl	15	108 (228)	625	25,000
			C-276	5,600 (2)
			C-22	7,100 (2), (3)
			ALLCORR®	15,000 (2), (3)
HCl	15	55 (131)	625	840
			C-276	280
			C-22	360 (3)
			ALLCORR®	710 (3)
HCl	10	104 (219)	625	36,000
			C-276	6,100 (3)
			C-22	11,000 (3)
			ALLCORR®	22,000 (2), (3)
$HCl + HNO_3$	28 17	109 (228)	625	> 99,000
			C-276	17,000 (3)
			C-22	2,000 (3)
			ALLCORR®	1,400 (2)

(1) Balance water (2) Intergranular corrosion (3) Welding seam corrosion

Table 71: Corrosion rates in HCl solutions [99]

Table 71 gives the results in HCl. The corrosion resistance is essentially determined by the amount of molybdenum contained in the alloy. The addition of 17 % HNO_3 considerably lowers the corrosion rate, particularly that of alloy ALLCORR®, which has the highest Cr content of 31 %. For the formic acid-sulphuric acid mixture, the low additions of HCl, HF, $FeCl_3$ and $CuCl_2$ increase the corrosion rate to different extents. It must be pointed out that, after the tests, many cases of intergranular corrosion and strong attack of the weld seam were found on the samples.

Investigations of various NiCrMo alloys for their possible use in supercritical water oxidation (SCWO) of organic waste is reported in [100]. This process is typically operated above the critical point of water (647 K (374 °C) and 221 bar for pure water). In the presence of compounds containing halogens and sulphur, the oxidation products are the corresponding acids, e.g. HCl, HF and H_2SO_4, in addition to CO_2 and H_2O. The materials listed in Table 72 were included in the investigation.

The tests were carried out in autoclaves in a mixture of water with 10 g/l dichloromethane (CH_2Cl_2) and 16 g/l H_2O_2 as the oxidising agent at a temperature of 693 K (420 °C) and a pressure of 400 bar. The test duration was 24 h. The mass losses of the samples for the 2 test runs are given in Table 73.

Material	UNS code	Cr	Ni %	Fe %	Al %	Mo %	W %	Others
G-30	N06030	29.4	40.1	14.5	–	5.1	2.9	Co, Cu
214	N07214	16.0	75.4	3.7	4.4	0.1	–	Zr, Cs*
602 CA		25.3	62.4	9.5	2.1	–	–	Ti
625	N06625	21.6	62.7	2.3	0.1	9.0	–	Ti
686	N06686	20.4	58.1	1.0	–	16.2	3.9	Ti

* in the commercially available variant, alloy 214 contains yttrium instead of caesium

Table 72: Composition of the investigated materials [100]

Material	Mass loss mg/cm^2	Mass loss mg/cm^2
G-30	2.8	2.9
214	26.6	–
214 preoxidised	50.8	39.9
602 CA	46.0-	–
602 CA preoxidised	15.5	–
625	–	33.5
686	73.3	23.8

Table 73: Mass losses of the samples after 24 h test period (2 test runs) [100]

According to this, only alloy G-30 can be expected to exhibit satisfactory corrosion behavior under SCWO conditions. The other alloys already show unacceptably high corrosion rates after 24 h.

A 30 Nickel-copper alloys

Nickel-copper alloys, e.g. Monel® Alloy 400 (UNS N04400, corresp to. DIN-Mat. No. 2.4360, 2.4366) exhibit lower resistance in hydrochloric acid than nickel itself. Some older data on the behavior of Monel® in different hydrochloric acid solutions at different temperatures is given in [47].

A 31 Nickel-molybdenum alloys

The NiMo alloy B-2 (UNS N10665, corresp. to. DIN-Mat. No. 2.4617), which has a low carbon content, was developed as a new version of the older grade alloy B (UNS N10001, corresp. to. DIN-Mat. No. 2.4800, 2.4810) especially for applications where there is exposure to hydrochloric acid. Newer variants are the grades alloy B-3 (UNS N10675) and alloy B-4 (UNS N10629) with improved thermal stability. Figure 72 shows an isocorrosion diagram for the grade B-2 [68]. Because the solubility of oxygen and thus the corrosion rate decreases at higher temperatures, there is a second line for the corrosion rate of 0.13 mm/a (5 mpy) at higher temperatures close to the boiling point.